Proc. Natl. Acad. Sci. USA
Vol. 92, pp. 8813–8817, September 1995
Physiology

α_1(E)-Catenin is an actin-binding and -bundling protein mediating the attachment of F-actin to the membrane adhesion complex

(cytoskeleton/uvomorulin/liver cell adhesion molecule/epithelial cell)

DAVID L. RIMM*, ERIKA R. KOSLOV, PARTOW KEBRIAEI, CAROL D. CIANCI, AND JON S. MORROW

Department of Pathology, Yale University School of Medicine, 310 Cedar Street, New Haven, CT 06510

Communicated by Edward Adelberg, New Haven, CT, June 19, 1995

ABSTRACT **Calcium-dependent homotypic cell–cell adhesion, mediated by molecules such as E-cadherin, guides the establishment of classical epithelial cell polarity and contributes to the control of migration, growth, and differentiation. These actions involve additional proteins, including α- and β-catenin (or plakoglobin) and p120, as well as linkage to the cortical actin cytoskeleton. The molecular basis for these interactions and their hierarchy of interaction remain controversial. We demonstrate a direct interaction between F-actin and α(E)-catenin, an activity not shared by either the cytoplasmic domain of E-cadherin or β-catenin. Sedimentation assays and direct visualization by transmission electron microscopy reveal that α_1(E)-catenin binds and bundles F-actin *in vitro* with micromolar affinity at a catenin/G-actin monomer ratio of ≈1:7 (mol/mol). Recombinant human β-catenin can simultaneously bind to the α-catenin/actin complex but does not bind actin directly. Recombinant fragments encompassing the amino-terminal 228 residues of α_1(E)-catenin or the carboxyl-terminal 447 residues individually bind actin in cosedimentation assays with reduced affinity compared with the full-length protein, and neither fragment bundles actin. Except for similarities to vinculin, neither region contains sequences homologous to established actin-binding proteins. Collectively these data indicate that α_1(E)-catenin is a novel actin-binding and -bundling protein and support a model in which α_1(E)-catenin is responsible for organizing and tethering actin filaments at the zones of E-cadherin-mediated cell–cell contact.**

E-cadherin and a group of tightly associated cytoplasmic proteins called α- and β-catenin (plakoglobin) and p120 mediate homotypic cell–cell adhesion (1–5), transmembrane control of adhesion (6, 7), surface domain topography (8), and possibly even some forms of heterotypic adhesion (9). How this cadherin-mediated adhesion complex links to the cortical actin skeleton remains uncertain. The largest component of this complex, α-catenin [previously called CAP102 (10)], has been postulated to link the membrane to F-actin, since E-cadherin–catenin complexes do not bind DNase I after detergent extraction of α-catenin (11). However, direct evidence for an interaction with actin is lacking, and a comparison of the derived amino acid sequence of α_1(E)-catenin† (12) displays no regions with obvious homology to other actin-binding sequence motifs (13–16).

In the present study, the association of α(E)-catenin with F-actin is explored by immunofluorescence microscopy of sparse epithelial cell cultures and with a series of purified recombinant α_1(E)-catenin peptides. Antibodies raised to recombinant α_1(E)-catenin reveal a coincident distribution of this protein with F-actin during early stages of cell–cell contact in cultured Madin–Darby canine kidney (MDCK) cells. *In vitro* assays indicate that α_1(E)-catenin binds and bundles F-actin with micromolar affinity and a fixed stoichiometry. Collectively, these studies establish a molecular mechanism for the attachment and organization of actin filaments at the cadherin-mediated cell adhesive junction and identify α_1(E)-catenin as a member of a class of actin-binding proteins. Portions of this work have been presented in abstract form (17).

MATERIALS AND METHODS

Preparation and Purification of Recombinant Proteins. All molecular biological techniques followed standard procedures (18) unless otherwise noted. Constructs were prepared using the pGEX (Pharmacia) prokaryotic expression vectors (19, 20), and expressed as glutathione *S*-transferase (GST) fusion proteins in either the HB101 or CAG456 strain of *Escherichia coli*. The latter strain, a derivative of a protease-deficient line, was used to minimize degradation of the fusion protein products (21). Bacterial cultures were grown for 3 hr and then induced for 1–3 hr with isopropyl β-D-thiogalactopyranoside before harvesting. Lysis was achieved by four repetitions of a 30-sec sonication on ice in TBSE (20 mM Tris·HCl, pH 8/0.1 mM PefablocSC (CentraChem, Stamford, CT)/150 mM NaCl/1 mM EDTA), with 1 mM dithiothreitol (DTT). The 15,000 × *g* supernatant of the lysate was affinity purified on glutathione-agarose (Sigma) at 4°C and washed extensively with TBSE before elution in TBSE containing 5 mM glutathione (Sigma) with 20 mM DTT on ice. The eluted material was enriched with PefablocSC (to 1 mM) before dialysis into TBSE containing 1 mM DTT. Most analyses were carried out by using the peptides as fusion proteins with GST. When required, GST sequences were removed by proteolysis with thrombin while the proteins were bound to the affinity matrix. For all of the analyses reported in this study, the presence or absence of the GST fusion sequences did not alter the activity of the peptides in any assay.

Actin Binding Assay. These assays used chicken skeletal muscle actin (a gift from Mark Mooseker, Yale University) as before (22). Actin was stored in buffer G (2 mM Tris·HCl, pH 8/0.2 mM ATP/0.2 mM $CaCl_2$/0.5 mM DTT/0.2% NaN_3). Fifteen minutes before use, the actin was polymerized by dilution at room temperature to 1.4–2.5 μM with polymerization buffer F (20 mM Tris·HCl, pH 7.4/75 mM KCl/10 mM NaCl/2 mM DTT/2.5 mM $MgCl_2$) (exact final actin concentrations for each experiment are given in the figure legends). Recombinant fusion proteins in F buffer were cleared at 100,000 × *g* for 30 min and allowed to interact with the actin for 15–30 min at room temperature prior to centrifugation at

The publication costs of this article were defrayed in part by page charge payment. This article must therefore be hereby marked "*advertisement*" in accordance with 18 U.S.C. §1734 solely to indicate this fact.

Abbreviation: GST, glutathione *S*-transferase.

*To whom reprint requests should be addressed.

†The nomenclature of α-catenin used here follows previous convention, in which alternative transcripts are designated by numeric subscript, while different members of the superfamily are referenced by letter (12). The α_1(E)-catenin used in this study thus represents alternative transcript 1 of the epithelial form (E) of α-catenin.

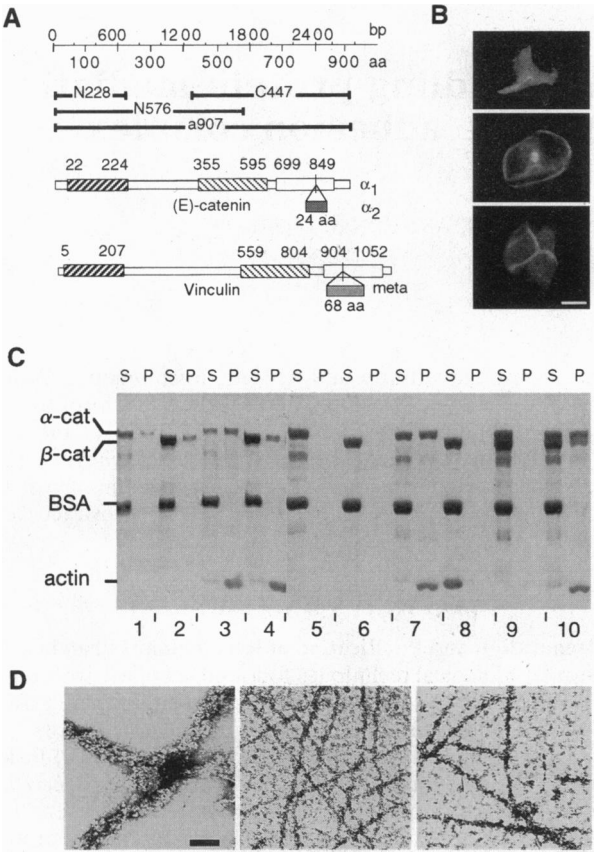

FIG. 1. α(E)-Catenin binds and bundles F-actin. (*A*) Schematic representation of the α(E)-catenin gene and its relationship to the peptides prepared for this study. Full-length cDNA of α_1(E)-catenin encodes a protein of 907 amino acids (a907). Constructs encoding the amino-terminal 228 residues (N228), the amino-terminal 576 residues (N576), or the carboxyl-terminal 447 residues (C447) were prepared by cloning or by restriction enzyme digestion of the full-length cDNA for α(E)-catenin (12). Represented at the top are nucleotide (bp) and amino acid (aa) positions. A schematic representation of the derived amino acid sequence of two isoforms of α(E)-catenin (12) and vinculin are also depicted. The hatched areas represent the regions of greatest homology between these proteins; the site of alternative mRNA splicing that distinguishes α_1(E)-catenin from α_2(E)-catenin at codon 812 occurs in a position similar to the alternative splice site in meta-vinculin. Homologous domains in α-catenin and vinculin are depicted by like hatching. Recombinant proteins representing the cytoplasmic domain (151 amino acids) of human E-cadherin (24) and human β-catenin (unpublished data) were also prepared. In general, all constructs were initially evaluated as fusion proteins with GST; the results of each assay were then confirmed by using peptides in which the GST sequences had been removed by proteolysis with thrombin (see *Materials and Methods*). (*B*) Representative fluorescence micrographs of three-cell clusters stained for E-cadherin (*Top*), F-actin (*Middle*), and α(E)-catenin (*Bottom*) demonstrate early and coincident assembly of these three proteins at zones of cell–cell contact. *Top* and *Middle* are double immunofluorescence micrographs; *Bottom* is from a comparable cell cluster. Maturation of the cadherin-based adhesive junction continues for >48 hr (25, 26); during the first 12–18 hr in culture, contact-naive MDCK cells display a graded hierarchy in the timing of cadherin, αIIβII spectrin (fodrin), and ankyrin assembly at zones of cell–cell contact (27). In no instance within the time scale of these experiments could the patterns of staining of these three proteins along the zones of cell–cell contact be distinguished. (Bar = 10 μM.) (*C*) The ability of α(E)-catenin (≈7 μM) or β-catenin (≈8 μM) to bind F-actin (2.2 μM) was examined *in vitro* by cosedimentation assay at either 100,000 × *g* (lanes 1–4) or 10,000 × *g* (lanes 5–10). Pellet (P) and supernatant (S) fractions are shown after SDS/PAGE. Neither protein sedimented appreciably in the absence of F-actin (lanes 1, 2, 5, 6, and 9). At 100,000 × *g*, ≈60% of the α(E)-catenin sedimented with F-actin (lane 3), whereas there was no change in the amount of β-catenin sedimented (lane 4). α(E)-Catenin also induced the sedimentation of F-actin at 10,000 × *g* (lane 7), again a property not shared by β-catenin (lane 8). When both α(E)- and β-catenin were present, both sedimented with F-actin (lane 10). Bovine serum albumin (BSA) at ≈2 mM was added to each sample prior to sedimentation as a marker of the purity of separation between supernatant and pellet fractions. All proteins shown here were used as GST fusion peptides. (*D*) Only full-length α_1(E)-catenin bundles F-actin filaments. Solutions of F-actin (2.5 μM) and the various catenin peptides were fixed in 0.2% glutaraldehyde and stained with 1% aqueous uranyl acetate for negative-stain electron microscopy. (*Left*) F-actin with a907 peptide. (*Center*) F-actin with N576 peptide. (*Right*) F-actin with N447 peptide. (Bar = 100 nm.)

100,000 × *g* or 10,000 × *g* for 30 min at 20°C in a Beckman 42.2Ti rotor. Comparable amounts of supernatant and pellet fractions were analyzed by densitometric scanning of Coomassie blue-stained SDS/polyacrylamide gels. Multiple dilutions were analyzed and compared with standard samples to establish instrumental linearity and to correlate OD with the amount of protein in each gel band. Binding affinities and stoichiometry were determined by nonlinear regression analysis.

Immunofluorescence Microscopy. Contact-diminished MDCK cells were generated by successive platings at low density, after which they were grown for up to 18 hr on either chamber slides (Nunc) or glass coverslips. For staining, cells were fixed for 20 min on ice with 1.75% formaldehyde in phosphate-buffered saline (PBS), permeabilized with 0.5% Triton X-100 in PBS at room temperature for 10 min, blocked for 1 hr with 5% bovine serum albumin in PBS, and then stained. Alternatively, cells were permeabilized and fixed on ice with methanol, blocked with 3% albumin at room temperature for 30 min, and then stained. Affinity-purified antibodies to either human E-cadherin (23), dog liver cell adhesion molecule (L-CAM) (a gift from Bruce Cunningham, Scripps Institute), or human α(E)-catenin (23) were diluted 1:100 to 1:500 prior to a 30-min incubation with the cells at room temperature. Bound antibodies were visualized with fluorescein-labeled with goat anti-rabbit IgG (Pierce). The distribution of F-actin was discerned by staining with rhodamine-labeled phallodin (Molecular Probes). Samples were visualized with a Nikon or Zeiss epifluorescence microscope and photographed with 35-mm Kodak Ektachome-1600 film. Film images were digitized with a BarneyScan scanner, cropped, and converted to gray scale with ADOBE PHOTOSHOP 2.5 on a Macintosh computer, and printed for publication with a Fuji color printer. All images are presented as recorded, without digital enhancement or filtering.

Electron Microscopy. Complexes of proteins were produced as described above for sedimentation and pipetted onto carbon–parlodion grids, fixed in 0.2% glutaraldehyde, and stained with aqueous 1% uranyl acetate. Grids were examined and photographed on a Zeiss CEM 910 transmission electron microscope.

Other Procedures. Protein concentrations were measured by the Bradford assay (Bio-Rad) with bovine γ-globulin as a standard. This method was calibrated against a known amount of α_1(E)-catenin determined by triplicate amino acid analysis at the Yale Protein Chemistry facility. The antibodies to human E-cadherin and α_1(E)-catenin have been described (23).

RESULTS

α(E)-Catenin and F-Actin Are Codistributed at Zones of Cell–Cell Contact. To understand the molecular basis for the interaction of the adhesion complex with actin, the cytoplasmic domains of human E-cadherin, α(E)-catenin, and β-catenin were each prepared as recombinant proteins in *E. coli*. Their ability to codistribute with F-actin during the early steps of cell–cell contact in cultured MDCK cells and to cosediment

with F-actin in sedimentation assays was measured. Also prepared was a series of peptides representing various subdomains of α(E)-catenin (Fig. 1*A*). The relationships of α- and β-catenin assembly to E-cadherin and F-actin assembly during the early steps in the formation of the cell–cell adhesive junction were surveyed by monitoring which proteins assembled at zones of cell–cell contact in sparse cultures of MDCK cells (Fig. 1*B*). While no attempt was made to capture the very earliest events in the assembly process as has been done by time-lapse video microscopy (28), examples of two-cell and three-cell clusters making contact early in sparse cultures were taken as representative of early productive assembly events. These studies demonstrated that the distribution of cortical F-actin at zones of initial cell–cell contact was strikingly coincident with the distribution of E-cadherin and α-catenin (Fig. 1*B*) as well as β-catenin (data not shown).

α(E)-Catenin Binds and Bundles F-Actin *In Vitro*. The various peptides were then examined for their ability to interact individually and collectively with F-actin *in vitro* by measuring their cosedimentation with F-actin. The cytoplasmic domain of E-cadherin did not sediment with F-actin under any circumstances (data not shown). α(E)-Catenin peptide a907 did cosediment with F-actin at both 100,000 × *g* and 10,000 × *g*, but β-catenin did not (Fig. 1*C*). However, β-catenin did sediment in the presence of α-catenin. In assays carried out at 10,000 × *g*, α(E)-catenin also stimulated the low-speed sedimentation of F-actin (Fig. 1*C*). These findings were not an artifact of the GST fusion sequence on the recombinant peptides, since proteolytic removal of GST had no effect on any of these activities, nor did the other GST-containing peptides induce the low-speed sedimentation of actin. Collectively, these results indicate that α(E)-catenin can directly bind F-actin and simultaneously mediate the attachment of β-catenin to an α(E)-catenin/F-actin complex.

The ability of α(E)-catenin peptide a907 to enhance the sedimentation of F-actin at 10,000 × *g* and its strong binding affinity for actin (see below) suggested that it may crosslink actin filaments into bundles. To verify this, mixtures of F-actin with α(E)-catenin peptide a907 and other peptides representing fragments of α(E)-catenin (Fig. 1*A*) were examined by electron microscopy (Fig. 1*D*). Peptide a907 induced large crosslinked actin filament clusters and branching bundles. Indistinct decorations could also be discerned along the bundled filaments, and in some areas these appeared in a periodic array, presumably representing bound peptide a907. Only singular filaments indistinguishable from control actin filaments characterized actin mixtures with the other peptides (Fig. 1*D* and data not shown).

α_1(E)-Catenin Binds F-Actin with Fixed Stoichiometry and Micromolar Affinity. To better characterize the interaction of α(E)-catenin with F-actin, increasing concentrations of peptide a907 were incubated with F-actin and the extent of binding was measured by densitometry after sedimentation at 100,000 × *g* (Fig. 2*A*). Also measured in these experiments was the amount of actin sedimented, as well as the level of free a907 in the supernatant. The ratio of the a907 peptide to actin in the pellet was used to estimate the extent of binding. These results demonstrated an apparent equilibrium dissociation constant (K_d) of 0.3 ± 0.4 μM and a capacity (B_{max}) of 0.16 ± 0.10 mol of catenin per mol of actin monomer. This stoichiometry corresponds to one molecule of α(E)-catenin for every six or seven actin monomers, close to the theoretical stoichiometry of 1:7 that would be expected for a dimeric protein linking two actin filaments [with a helical repeat unit containing 14 actin monomers (29)]. Hill analysis of the binding data yielded a coefficient of 0.84 ± 0.22, indicating a lack of binding cooperativity. The salt dependence of α(E)-catenin's actin-binding and -bundling activity demonstrated an approximately inverse linear dependence of a907 binding to F-actin at ionic strengths of 100–500 mM (Fig. 2*B*). The ability of a907 to induce the

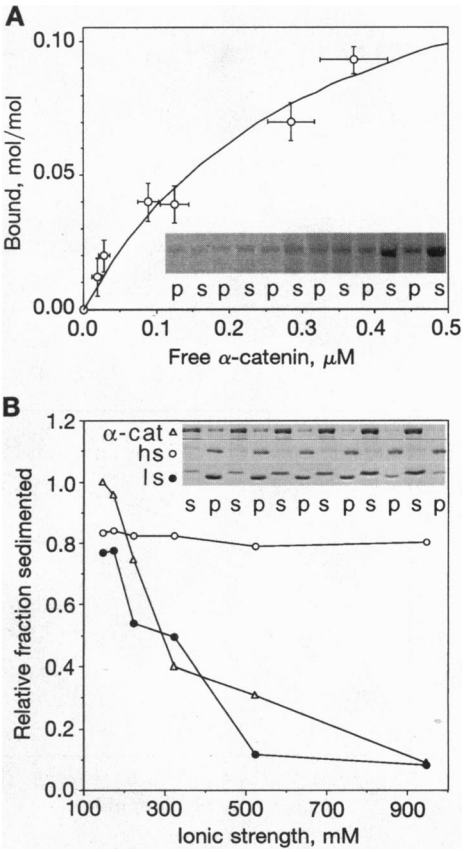

FIG. 2. Binding of α_1(E)-catenin to F-actin is saturable. (*A*) Increasing concentrations of full-length α_1(E)-catenin a907 were incubated with 1.4 μM F-actin in buffer F with 50 mM KCl and 10 mM NaCl at 4°C and sedimented at 100,000 × *g*. Each pair of lanes in the *Inset* represents the pellet (p) and supernatant (s) fractions from one determination. Less than 7% of the actin failed to sediment in these experiments, and actin loading was constant between lanes (data not shown). The binding was quantified by densitometry. Nonlinear regression analysis indicated that α_1(E)-catenin bound actin with an apparent K_d = 0.3 ± 0.4 μM and B_{max} = 0.16 ± 0.10 mol of catenin per mol of actin monomer. The Hill coefficient for this binding was 0.84 ± 0.22 (plot not shown), indicating a lack of cooperativity. All error estimates are ±2 SD. Each point represents the average of at least three separate determinations. (*B*) Binding of α_1(E)-catenin a907 (Δ) (≈4 μM) to F-actin (2.2 μM) was compared at various ionic strengths in the same binding buffer used above. For these experiments, increased ionic strength was obtained by the addition of NaCl to the indicated final total ionic strengths. Also compared in this experiment was the effect of ionic strength on the sedimentation of F-actin at 100,000 × *g* [high speed (hs), ○] and at 10,000 × *g* [low speed (ls), ●], a measure of bundling activity. Note the coincident decline of the binding and bundling curves with increasing ionic strength, without a change in the sedimentation of F-actin at 100,000 × *g*.

bundling of actin paralleled its binding behavior, whereas there was no change in the state of F-actin over this range of ionic strength (as measured by sedimentation at 100,000 × *g*). The direct binding of α(E)-catenin to actin thus fully accounts for its bundling activity, an effect manifested over a physiologic range of ionic strength.

Recombinant Peptides Representing Both Ends of α-Catenin Bind Actin *In Vitro*. The interaction of peptides representing either the amino-terminal 228 residues (N228) or the carboxyl-terminal 447 residues (C447) of α(E)-catenin with actin was also examined (Fig. 3). The N228 peptide tended to aggregate at concentrations exceeding ≈2 μM, and measurements of its affinity for F-actin must therefore be considered tentative. Nevertheless, both peptides bound F-actin with micromolar affinity, suggesting that both ends of α(E)-catenin

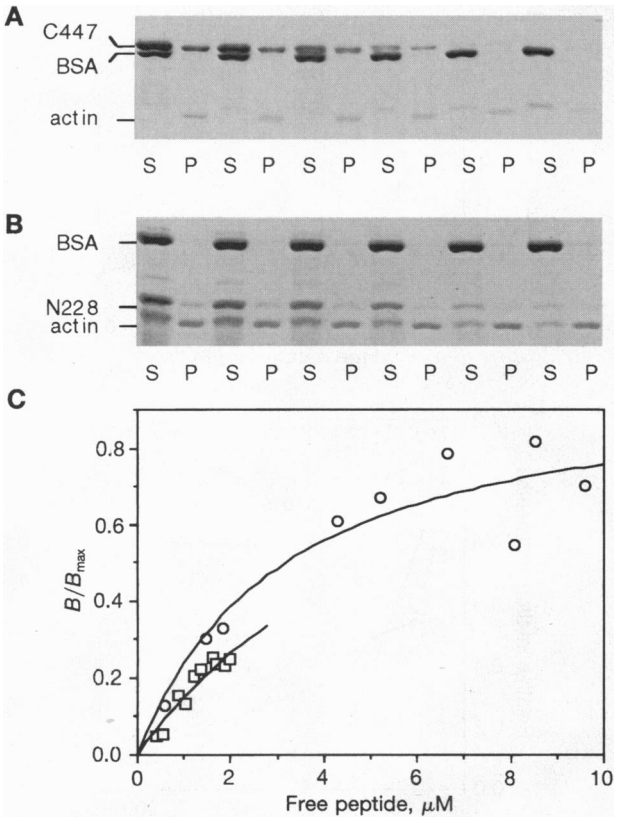

FIG. 3. Both termini of α_1(E)-catenin can bind F-actin. Various concentrations of either the C447 peptide (*A*) or the N228 peptide (*B*) were incubated as GST fusion proteins under binding conditions with F-actin ($\approx$2 μM) and sedimented at 100,000 $\times$ *g*. Neither peptide alone induced the sedimentation of F-actin at 10,000 $\times$ *g* (data not shown). GST alone did not sediment with actin under any conditions (data not shown), nor did other unrelated fusion peptides incorporating GST. No subtraction of background binding was therefore indicated. (*A* and *B*) SDS/PAGE analysis of the binding. BSA represents bovine serum albumin that was added to the solutions ($\approx$2–3 μM) during the incubation as a calibration marker and as a measure of the purity of the pellet fraction (from which should be absent). Each pair of lanes shows the supernatant (S) and pellet (P) fractions. All gels were stained with Coomassie blue. (*C*) Quantitation of the binding indicates that each peptide binds F-actin with micromolar affinity. For the C447 peptide (○), the estimated K_d = 3.2 $\pm$ 3.1 μM. The N228 peptide (□) displayed a binding isotherm suggestive of a $K_d \approx 5.5 \pm 10.6$ μM, although the limited range of concentrations of N228 that could be explored due to its aggregation at higher concentrations and susceptibility to degradation rendered more precise estimates inaccessible, and its saturability could therefore not be confirmed.

may participate in actin binding. While the minimal sequences required for actin binding α(E)-catenin have not been defined, it is noteworthy that none of 12 different known actin-binding motifs, including those in other actin-crosslinking and/or -bundling proteins such as villin, gelsolin, α-actinin, spectrin, and dystrophin, shares significant similarities to any region in α(E)-catenin, although similarities do exist to the actin-binding site recently identified in a homologous carboxyl-terminal region of vinculin, residues 893–1016 (30, 31).

DISCUSSION

We conclude that α_1(E)-catenin is an actin-binding and -bundling protein that organizes, attaches, and presumably recruits filamentous actin to zones of E-cadherin-mediated cell–cell contact. This conclusion rests on four lines of evidence: (*i*) recombinant α_1(E)-catenin and recombinant peptides encompassing either its amino-terminal 228 residues or its carboxyl-terminal 447 residues all sediment with F-actin at 100,000 $\times$ *g*; (*ii*) dimers of full-length α_1(E)-catenin, but not the shorter peptides, induce the low-speed sedimentation of F-actin; (*iii*) only full-length α_1(E)-catenin creates bundled actin filaments visualized by negative-stain electron microscopy; and (*iv*) there is early coassembly of E-cadherin, F-actin, and α(E)-catenin at points of cell–cell contact in sparse cultures of MDCK cells. Although the stoichiometry of α_1(E)-catenin binding to actin suggests that it acts as a dimer, the significance of α_1(E)-catenin dimerization or whether it is required for actin-bundling activity is unknown. However, with studies that indicate that β-catenin binds both the cytoplasmic domain of E-cadherin and that of α-catenin (32, 33), a detailed model of the molecular architecture of the cadherin-based cell–cell adhesion complex emerges. In this model, β-catenin, perhaps under the control of Wnt-1, mediates the attachment of E-cadherin to α(E)-catenin (33), which in turn mediates the attachment and organization of F-actin at adherens junctions and other zones of cadherin-mediated cell–cell contact.

The actin-binding sites identified here are conserved in both of the known isoforms of α(E)-catenin (12) and represent novel actin-binding motifs based on sequence homologies. While the minimal actin-binding motif in α(E)-catenin has not been defined, it is noteworthy that none of 12 different known actin-binding motifs, including those in other actin-crosslinking and/or -bundling proteins such as villin, gelsolin, α-actinin, spectrin, and dystrophin, shares significant similarities to any region in α(E)-catenin. A 17-amino acid region, residues 64–80, shows some similarity (20–30%) to the actin-binding domain found in α-actinin, filamin, dystrophin, and spectrin. However, the residues most highly conserved in this motif, including a hydrophobic 7-amino acid sequence critical for interaction with F-actin, are not conserved in α(E)-catenin (34), and the region of homology spans only half of the region required for actin binding in filamin (35).

Although α(E)-catenin and vinculin are both members of the same gene superfamily and share many homologies overall, they appear to interact with actin differently. Unlike α(E)-catenin, vinculin does not crosslink F-actin. Recently, an F-actin binding site has been identified in the homologous carboxyl-terminal region of vinculin, residues 893–1016 (30), and this site is modulated by sequences near the amino terminus of vinculin (31). However, actin-binding activity has not been found in the amino-terminal region of vinculin, even in sequences that share 48% similarity and 27% identity with α(E)-catenin. It is interesting to speculate that the actin-binding domains identified here in the "head" and "tail" domains of α(E)-catenin interact positively to augment actin binding, in a manner similar to the way the head and tail interactions downregulate actin binding in vinculin. This possibility might be inferred from the data, since the affinity of full-length α(E)-catenin for actin is nearly an order of magnitude greater than for either the N228 or the C447 peptide alone. It will be important to determine whether the amino- and carboxyl-terminal actin-binding domains identified here act independently or whether they interact to create a single site of higher affinity in the native protein.

We thank Mr. Paul Stabach and Dr. Chris Lombardo for expert advice and assistance with cloning, sequencing, and the preparation of recombinant peptides. Support for this work was provided by grants from the National Institutes of Health (RO1-DK43812 and PO1-DK38979) to J.S.M. and by a Crohn's and Colitis Foundation Career Development Award to D.L.R.

1. Reynolds, A. B., Daniel, J., McCrea, P. D., Wheelock, M. J., Wu, J. & Zhang, Z. (1994) *Mol. Cell. Biol.* **14,** 8333–8342.
2. Takeichi, M. (1991) *Science* **251,** 1451–1455.
3. Kemler, R. (1993) *Trends Genet.* **9,** 317–321.
4. Gumbiner, B. M. & McCrea, P. D. (1993) *J. Cell Sci. Suppl.* **17,** 155–158.

5. Hinck, L., Näthke, I. S., Papkoff, J. & Nelson, W. J. (1994) *Trends Biochem Sci.* **19,** 538–542.
6. Friedlander, D. R., Mége, R.-M., Cunningham, B. A. & Edelman, G. M. (1989) *Proc. Natl. Acad. Sci. USA* **86,** 7043–7047.
7. Nagafuchi, A. & Takeichi, M. (1989) *Cell Regul.* **1,** 37–44.
8. Nelson, W. J. & Hammerton, R. W. (1989) *J. Cell Biol.* **108,** 893–902.
9. Cepek, K. L., Shaw, S. K., Parker, C. M., Russell, G. J., Morrow, J. S., Rimm, D. L. & Brenner, M. B. (1994) *Nature (London)* **372,** 190–193.
10. Nagafuchi, A., Takeichi, M. & Tsukita, S. (1991) *Cell* **65,** 849–857.
11. Ozawa, M., Ringwald, M. & Kemler, R. (1990) *Proc. Natl. Acad. Sci. USA* **87,** 4246–4250.
12. Rimm, D. L., Kebriaei, P. & Morrow, J. S. (1994) *Biochem. Biophys. Res. Commun.* **203,** 1691–1699.
13. Rozycki, M. D., Myslik, J. C., Schutt, C. E. & Lindberg, U. (1994) *Curr. Opin. Cell Biol.* **6,** 87–95.
14. Vandekerckhove, J. & Vancompernolle, K. (1992) *Curr. Opin. Cell Biol.* **4,** 36–42.
15. Way, M., Pope, B. & Weeds, A. (1991) *J. Cell Sci. Suppl.* **14,** 91–94.
16. Hartwig, J. H. & Kwiatkowski, D. J. (1991) *Curr. Opin. Cell Biol.* **3,** 87–97.
17. Rimm, D. L., Kabriaei, P. & Morrow, J. S. (1994) *Mol. Biol. Cell* **5,** Suppl., 5 (abstr.).
18. Sambrook, J., Fritsch, E. F. & Maniatis, T. (1989) *Molecular Cloning: A Laboratory Manual* (Cold Spring Harbor Lab. Press, Plainview, NY), 2nd Ed.
19. Smith, D. B. & Johnson, K. S. (1988) *Gene* **67,** 31–40.
20. Kennedy, S. P., Warren, S. L., Forget, B. G. & Morrow, J. S. (1991) *J. Cell Biol.* **115,** 267–277.
21. Baker, T. A., Grossman, A. D. & Gross, C. A. (1984) *Proc. Natl. Acad. Sci. USA* **81,** 6779–6783.
22. Mische, S. M., Mooseker, M. S. & Morrow, J. S. (1987) *J. Cell Biol.* **105,** 2837–2845.
23. Rimm, D. L., Sinard, J. H. & Morrow, J. S. (1995) *Lab. Invest.* **72,** 506–512.
24. Rimm, D. L. & Morrow, J. S. (1994) *Biochem. Biophys. Res. Commun.* **200,** 1754–1761.
25. Nelson, W. J., Hammerton, R. W., Wang, A. Z. & Shore, E. M. (1990) *Semin. Cell Biol.* **1,** 359–371.
26. Wollner, D. A., Krzeminski, K. A. & Nelson, W. J. (1992) *J. Cell Biol.* **116,** 889–899.
27. Morrow, J. S., Cianci, C. D., Kennedy, S. P. & Warren, S. L. (1991) in *Ordering the Membrane Cytoskeleton Trilayer*, eds. Mooseker, M. S. & Morrow, J. S. (Academic, New York), pp. 227–244.
28. McNeill, H., Ryan, T. A., Smith, S. J. & Nelson, W. J. (1993) *J. Cell Biol.* **120,** 1217–1226.
29. Huxley, H. E. & Brown, W. (1967) *J. Mol. Biol.* **30,** 383–434.
30. Menkel, A. R., Kroemker, M., Bubeck, P., Ronsiek, M., Nikolai, G. & Jockusch, B. M. (1994) *J. Cell Biol.* **126,** 1231–1240.
31. Johnson, R. P. & Craig, S. W. (1995) *Nature (London)* **373,** 261–264.
32. Hinck, L., Nelson, W. J. & Papkoff, J. (1994) *J. Cell Biol.* **124,** 729–741.
33. Aberle, H., Butz, S., Stappert, J., Weissig, H., Kemler, R. & Hoschuetzky, H. (1994) *J. Cell Sci.* **107,** 3655–3663.
34. Matsudaira, P. (1991) *Trends Biochem. Sci.* **16,** 87–92.
35. Lebart, M. C., Mejean, C., Casanova, D., Audemard, E., Derancourt, J., Roustan, C. & Benyamin, Y. (1994) *J. Biol. Chem.* **269,** 4279–4284.